JOURNAL OF COLLOID AND INTERFACE SCIENCE **184,** 550–563 (1996)
ARTICLE NO. 0651

Surface Tension of Aqueous Solutions of Electrolytes: Relationship with Ion Hydration, Oxygen Solubility, and Bubble Coalescence

PETER K. WEISSENBORN[1] AND ROBERT J. PUGH

Institute for Surface Chemistry, Thin Films Group, Box 5607, S-114 86 Stockholm, Sweden

Received February 23, 1996; accepted July 22, 1996

The surface tension of aqueous solutions of simple inorganic electrolytes (36 in total) have been measured by the maximum bubble pressure method as a function of electrolyte concentration up to 1 *M*. In most cases the surface tension increased, however in a minority of cases, certain combinations of cations and anions had a negligible effect or decreased surface tension. Results were analysed in terms of surface tension/electrolyte concentration gradients ($d(\Delta\gamma)/dc$) and this parameter was found to correlate with the entropies of ion hydration, Jones–Dole viscosity coefficients and dissolved oxygen gradients. Calculation of Gibbs surface deficiencies for selected electrolytes were carried out using the raw surface tension data. Discussion of the surface tension/electrolyte concentration gradients was extended to the mechanism of inhibition of bubble coalescence by electrolytes. The Gibbs–Marangoni effect did not provide a satisfactory explanation for the inhibition of coalescence for all electrolytes and from the present study we suggest that dissolved gas (microbubble) gradients between macroscopic bubbles plays an important role in the coalescence process.

Key Words: **surface tension; electrolytes; bubble coalescence; dissolved gases.**

INTRODUCTION

Investigations of the surface tension of electrolytes have been reported sporadically in the literature. Recently, surface tension data for over 60 inorganic electrolytes were tabulated (1). The majority of data were compiled from literature prior to the 1970s with very little discussion or evaluation of the data. More critical discussion of results from surface tension measurements on aqueous solutions of electrolytes has been given by other authors (2–5). The increase in surface tension of water upon addition of electrolyte has been explained by the repulsion or negative adsorption of ions from the gas/water interface. The surface deficiency of the electrolyte ($\Gamma_{el}^{H_2O}$) can be calculated by the Gibbs equation (with the Gibbs dividing plane chosen such that $\Gamma_{H_2O} = 0$)

$$\Gamma_{el}^{H_2O} = -\frac{1}{RT}\left(\frac{d\gamma}{d\ln a_{el}}\right)_T, \qquad [1]$$

where γ is surface tension, a_{el} is electrolyte activity, R is the gas constant, and T is temperature (6).

Onsager and Samaras (7) explained the surface deficiency of ions in terms of repulsive electrostatic image forces. Their theory was criticised due to its oversimplicity, mathematical treatment and neglection of structural (water) features (8), but nevertheless could partially account for increases in surface tension at low concentrations (<0.2 *M*) (2). Other authors (2, 9) were also critical of the Onsager–Samaras theory and argued that the effects of ions on water structure were more important than image forces. Aveyard and Saleem (4) showed that dispersion force theory gives a reasonably good fit to experimental data if allowance is made for an electrolyte free layer of water between the interface and electrolyte solution. Johansson and Eriksson (3) also used the concept of an electrolyte free layer. Hey *et al.* (5) have shown that for a selection of 1:1 electrolytes, the increase in surface tension is directly proportional to the enthalpy of hydration of ions indicating that ions prefer to be fully hydrated in the bulk solution rather than partially hydrated at the interface. Further, the more hydrated the ions the further they are displaced or the more water they displace from the interface.

Linked with the hydration of ions is the consequent decrease in dissolved gas concentration and we have recently shown a correlation between dissolved oxygen concentration and surface tension (10). Overall, the above literature strongly indicates that electrostatic image forces cannot solely account for the increase in surface tension. In addition, ion hydration, dispersion forces and dissolved gas concentration must be considered in any theory of electrolyte effects on surface tension, especially at higher electrolyte concentrations.

In the present study we have measured the surface tension of over thirty electrolytes in the concentration range 0 to 1 *M* using a relatively new, commercially available method for surface tension measurement. The maximum bubble

[1] To whom correspondence should be addressed.

0021-9797/96 $18.00

pressure method (MBPM) measures the pressure inside a bubble blown in solution (11). The method is based on the concept that bubble pressure is proportional to surface tension via Laplace's law. The advantage of this method over conventional methods such as the Wilhemy plate or Du Nöuy ring is that the bubble pressure (surface tension) is less sensitive to impurities or contamination. Also the method is quick and convenient.

Our aim was to investigate the effect of concentration of electrolyte on surface tension and correlate the values of $d(\Delta\gamma)/dc$ (where $\Delta\gamma$ is the change in surface tension relative to water and c is concentration) with the hydration of ions, dissolved oxygen concentration and assess the role of $d(\Delta\gamma)/dc$ in the coalescence of bubbles in electrolytes. Bubble coalescence in electrolyte solution has recently attracted much attention due to the phenomenological observations reported by Craig *et al.* (12). They reported that increasing the concentration of electrolytes (consisting of a certain combination of cation and anion) beyond a critical value gave a pronounced inhibition of coalescence. In addition to our previous paper (10), the results and discussion presented here offer a further explanation of this phenomenon.

EXPERIMENTAL

Stock solutions (2 *M*) of inorganic electrolytes were prepared in water. The electrolytes were of analytical reagent quality and, if available, of purity greater than 99.0 or 99.5%. Water was purified by a Milli-Q Plus 185 system. All glassware was cleaned in chromic acid, rinsed three times with Milli-Q water, and handled with gloves to avoid contamination.

Surface tension was measured using a SensaDyne 6000 tensiometer and version 4.0 software. The tensiometer uses dual capillaries which allow measurements to be made independent of solution height or volume (11). Glass capillaries of diameters 4.0 and 0.5 mm were used, and bubble pressure was measured at the small capillary. High-purity nitrogen was used to blow the bubbles. Calibration was carried out using Milli-Q water and NaCl (2 *M*), both of known surface tension (13). Surface tension of the electrolyte solutions was measured relative to water by measuring the surface tension of water and then adding stock electrolyte solution in selected increments to give surface tensions for at least five concentrations in the range 0.05 to 1 *M*. Temperature was maintained at room temperature (on average 24°C) to within ±0.2°C. A plot of the change in surface tension relative to water ($\Delta\gamma$) versus electrolyte concentration (c) gave the surface tension gradient ($d(\Delta\gamma)/dc$).

Typically about 30 to 100 bubbles, depending on the bubble interval, were blown and an average surface tension obtained. Because a new gas/water interface is generated with every bubble the MBPM is less sensitive to impurities or contamination than conventional methods. Nevertheless there was some concern over possible organic impurities in the reagents. Earlier workers (2, 3) using the Wilhemy plate method found it necessary to purify their reagents by roasting and re-crystallization to get reliable surface tensions of electrolyte solutions. To eliminate any doubt in our results the surface tension of solutions of KCl and NaBr were measured before and after roasting of the solids and no differences in $d(\Delta\gamma)/dc$ (within experimental error) were found. Since this comparison was not made for all solids, there is still a possibility that some samples (especially the acetate salts at high concentration) may contain impurities. Since almost all electrolytes tested gave a linear relationship between surface tension and concentration, we felt that the combination of the quoted reagent purity and method of surface tension measurement were adequate to give reliable values of $d(\Delta\gamma)/dc$.

The rate of bubble growth or bubble interval can also be controlled to give dynamic surface tensions, although this asset is more appropriate for studying diffusion limited adsorption of large molecules. Surface tension of all the electrolytes was, nevertheless, measured at two bubble intervals: 1.5 s (relatively slow) and 0.15 s (relatively fast). For selected electrolytes the effect of bubble interval on surface tension was measured over a wider range. The bubble interval was defined as the time in seconds between the detachment of bubbles from the small capillary, the reciprocal being bubbles per second. The reliable operating range for our instrument was from 2.5 s (0.4 bubbles s^{-1}) to 0.1 s (10 bubbles s^{-1}).

The precision of the bubble method was tested by measuring the surface tension of water, NaBr (1 *M*) and $MgSO_4$ (1 *M*) seven times, alternating between each solution, at a bubble interval of 1.5 s and 22.0°C. The mean surface tension of water was 72.37 mN m^{-1} with standard deviation of 0.03. The mean change in surface tension relative to water ($\Delta\gamma = \gamma - \gamma_0$, where γ_0 is for water) and standard deviation of NaBr and $MgSO_4$ were 2.06 ± 0.05 and 2.71 ± 0.05 mN m^{-1}, respectively.

RESULTS

Effect of Bubble Rate on Surface Tension

The ability to control the bubble interval with the maximum bubble pressure method allows differences between static (equilibrium) and dynamic surface tensions to be measured. At short bubble intervals, the lifetime of the surface active species at the interface is decreased (for positively adsorbed species), resulting in a dynamic surface tension. However, hydrodynamic effects also become significant at short bubble intervals and a false or enhanced dynamic surface tension may result due to a change in viscosity of the solution (14). Fainerman *et al.* (14) have corrected for vis-

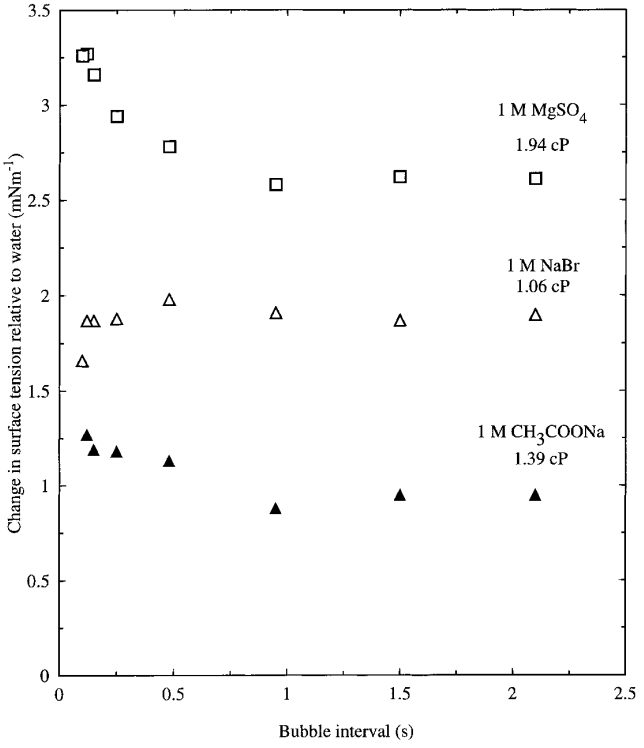

FIG. 1. Effect of absolute viscosity of electrolyte at 20°C and bubble interval on the change in surface tension relative to water. Note for CH_3COONa and $MgSO_4$ the deviation is positive and for NaBr it is negative. Viscosity for water is 1.002 cP at 20°C. Viscosities taken from ref. (13).

cosity effects for the measurement of surface tension of highly viscous solutions. Their maximum bubble pressure tensiometer uses a much narrower single capillary (0.0824 mm) and can control bubble size.

In order to investigate the influence of viscosity on surface tension, the change in surface tension relative to water ($\Delta\gamma$) for 1 *M* solutions of $MgSO_4$, CH_3COONa, and NaBr were determined over a range of bubble intervals. Figure 1 shows that in the range 1 to 2.5 s the surface tension is fairly constant, while at intervals less than 1 s the surface tension begins to deviate. At close to the shortest bubble interval attainable by the instrument (0.1 s) a significant change in surface tension was detected for $MgSO_4$. For CH_3COONa the change is less significant, and for NaBr the change is only apparent at 0.1 s and in the opposite direction to $MgSO_4$ and CH_3COONa.

A further indication of the effect of viscosity on surface tension can be illustrated by subtracting the $\Delta\gamma$ values obtained at the maximum and minimum range of bubble intervals in Fig. 1. This range was defined as $\Delta\gamma_{0.1s} - \Delta\gamma_{2.1s}$, where $\Delta\gamma_{0.1s}$ is $\Delta\gamma$ at a bubble interval of 0.1 s and $\Delta\gamma_{2.1s}$ is at 2.1 s. The results are shown in Table 1 along with the viscosities of the test solutions. From this data it would appear that the magnitude and deviation of $\Delta\gamma_{0.1s} - \Delta\gamma_{2.1s}$ from zero is dependent on the viscosity of the electrolytes relative to NaCl. For H_2O and NaCl (2 *M*) no changes occurred since these solutions were used as calibration standards at all bubble intervals.

TABLE 1
Effect of Electrolyte Viscosity on the Maximum Change in Surface Tension

Solution (molarity)	Absolue viscosity (cP at 20°C)	$\Delta\gamma_{0.1s} - \Delta\gamma_{2.1s}$ (mN m^{-1})
H_2O	1.002	0, calibration std
NaCl (2 *M*)	1.097	0, calibration std
NaBr (1 *M*)	1.057	−0.24
CH_3COONa (1 *M*)	1.394	0.32
$MgSO_4$ (1 *M*)	1.939	0.65

To investigate further the influence of viscosity on $\Delta\gamma$, the surface tension of all electrolytes used in this study were measured at bubble intervals of 1.5 and 0.15 s up to electrolyte concentrations of 1.0 *M*. Figure 2 shows that for most electrolytes there was a relatively small increase in $\Delta\gamma$ at 0.15 s and suggests the increase can be partly attributed to viscosity. Note, that this applies only to the Sensadyne instrument and the capillary diameter used (0.5 mm). The correlation coefficient (0.80) indicates that the increase may not solely depend on viscosity and that some other proper-

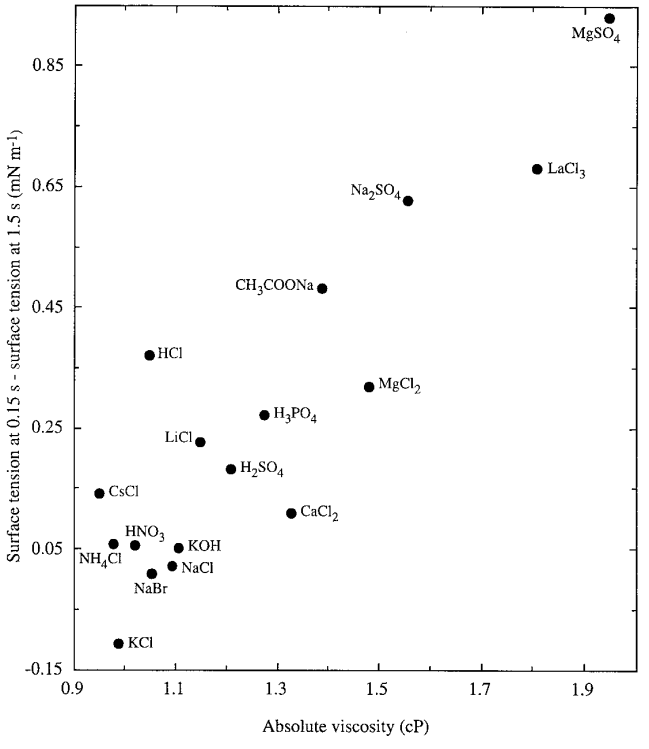

FIG. 2. Difference in surface tensions at bubble intervals 0.15 and 1.5 s ($\Delta\gamma_{0.15s} - \Delta\gamma_{1.5s}$) versus absolute viscosity for electrolytes at 1 *M* and 20°C. Viscosities taken from ref. (13). Correlation coefficient = 0.80.

ties, such as ion diffusion rate or impurities, may also affect $\Delta\gamma$ at short bubble intervals. Ion diffusion is expected to be sufficiently fast to not influence surface tension at a bubble interval of 0.15 s, but this needs to be investigated further before it can be ruled out as an influence.

To calculate the absolute values of surface tension (static or dynamic), corrections for solution viscosity need to be introduced when working with short bubble intervals. For the SensaDyne instrument in the current configuration, it was concluded from the above results that the effect of viscosity on surface tension measured at short bubble intervals only becomes significant (greater than experimental error) for solutions with viscosities above approximately 1.3 cP. The surface tension values measured at long bubble interval (1.5 s) were not affected by viscosity. This enabled the measurements at 1.5 s to be used to access the effect of electrolyte concentration on surface tension.

Effect of Electrolyte Concentration on Surface Tension

The effect of concentration (c = 0 to 1 M) of selected 1:1 and multivalent electrolytes on $\Delta\gamma$ is shown in Figs. 3 and 4, respectively. Straight lines of gradient $d(\Delta\gamma)/dc$ were fitted by least squares regression analysis. Values of $d(\Delta\gamma)/dc$ are shown in Table 2, along with literature values where available and $d(\Delta\gamma)/dc$ measured at bubble interval 0.15 s. Table 2 shows negative and positive values of $d(\Delta\gamma)/dc$. Negative values of $d(\Delta\gamma)/dc$ (decrease in γ) indicate positive surface excess concentrations of solute or positive adsorption of the solute at the gas/water interface. Positive values of $d(\Delta\gamma)/dc$ (increase in γ) indicate negative surface excess concentrations of solute or negative adsorption (depletion) of the solute from the gas/water interface (15). Negative or positive values of $d(\Delta\gamma)/dc$ do not necessarily mean that both cations and anions are positively or negatively adsorbed, but that one ion may dominate over the other in terms of overall adsorption and effect on surface tension.

To our knowledge, no such systematic experimental study at concentrations below 1 M has been reported. The majority of previously reported literature data in Table 2 (column 2) is for concentrations above 1 M with only a few measurements of surface tension below 1 M and were obtained by a variety of methods and experimentalists. While this does not detract from the reliability of a single measurement listed in column 2, it does not allow reliable comparisons between measurements and identification of trends. Comparison between our experimental values of $d(\Delta\gamma)/dc$ at 1.5 s and those from the literature verifies the trends between 1:1 electrolytes and electrolytes containing multivalent ions, but only in a few cases do actual values of $d(\Delta\gamma)/dc$ agree within experimental error. Our experimental results, because of the consistency in the overall experimental procedure, also allow relative comparison within groups of electrolytes (for example, 1:1 electrolytes with a common cation or anion).

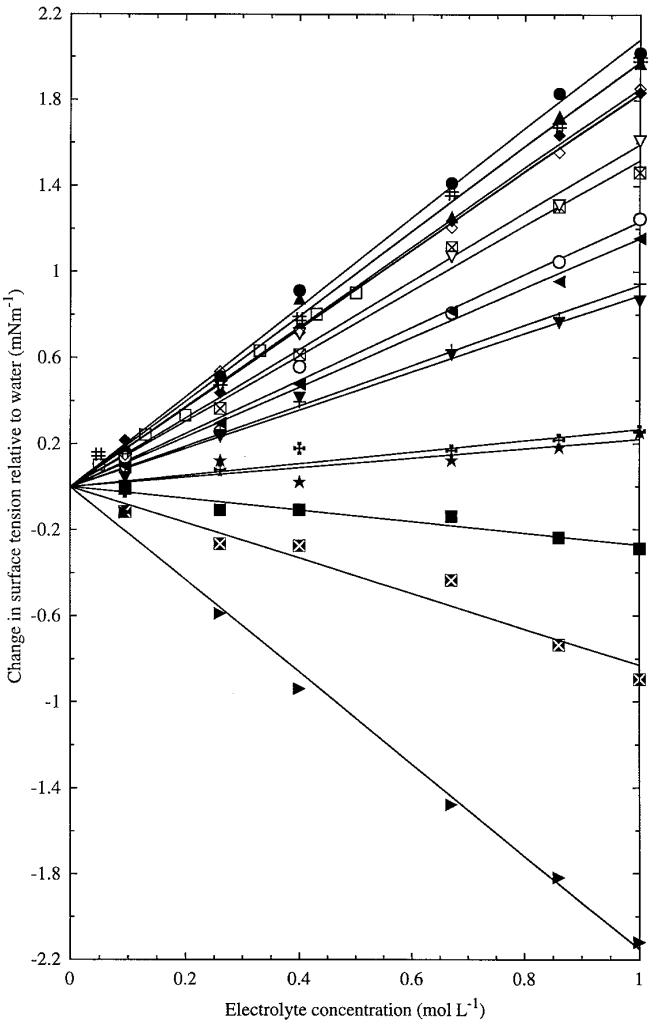

FIG. 3. Effect of electrolyte concentration on the change in surface tension relative to water for 1:1 electrolytes. Bubble interval, 1.5 s. Experimental error in data points is ±0.1 mN m^{-1}. HCl (■), LiCl (▲), NaCl (●), KCl (♦), CsCl (⊠), NaF (□), NaI (○), NH_4Cl (▽), NaBr (◇), HNO_3 (⊠), $(CH_3)_4NCl$ (+), NH_4NO_3 (◀), $HClO_4$ (▶), $NaClO_3$ (▼), $LiClO_4$ (✣), $NaClO_4$ (★), KOH (#).

DISCUSSION

Comparison between 1:1 and Multivalent Electrolytes

To make a comparison between the effects of 1:1 and multivalent electrolytes on $\Delta\gamma$, on a more thermodynamic basis, the concentration of selected electrolytes was expressed as activity and plotted against $\Delta\gamma$. Activities were calculated by converting molarity to molality and multiplying by the mean molal activity coefficient using the equations given by Robinson and Stokes (17). Solution densities and activity coefficients were taken from literature (13, 17, 18). Figure 5 shows that the multivalent electrolytes had the greatest effect on surface tension and confirms the earlier trends in Table 2 where larger values of $d(\Delta\gamma)/dc$ for

multivalent electrolytes were shown compared to the 1:1 electrolytes. To our knowledge, this is the first time surface tension data has been plotted against activity for such a wide range of different electrolytes and at low concentrations (down to approximately 0.05 *M*). The shape of the graphs shows distinct nonlinear behavior at low activities. However, at higher activities, more linear behavior was observed for almost all electrolytes and a straight line could be drawn through the last three data points.

Attempts were made to calculate the surface deficiency or excess for each electrolyte in Fig. 5. Values of $d(\Delta\gamma)/d \ln a$ were obtained by drawing tangents to each data point in Fig. 5 and the surface deficiency or excess calculated using Eq. [1] (Gibbs's equation). A plot of $\Gamma_{el}^{H_2O}$ versus *a* was drawn (Fig. 6 shows results for some chloride salts) and

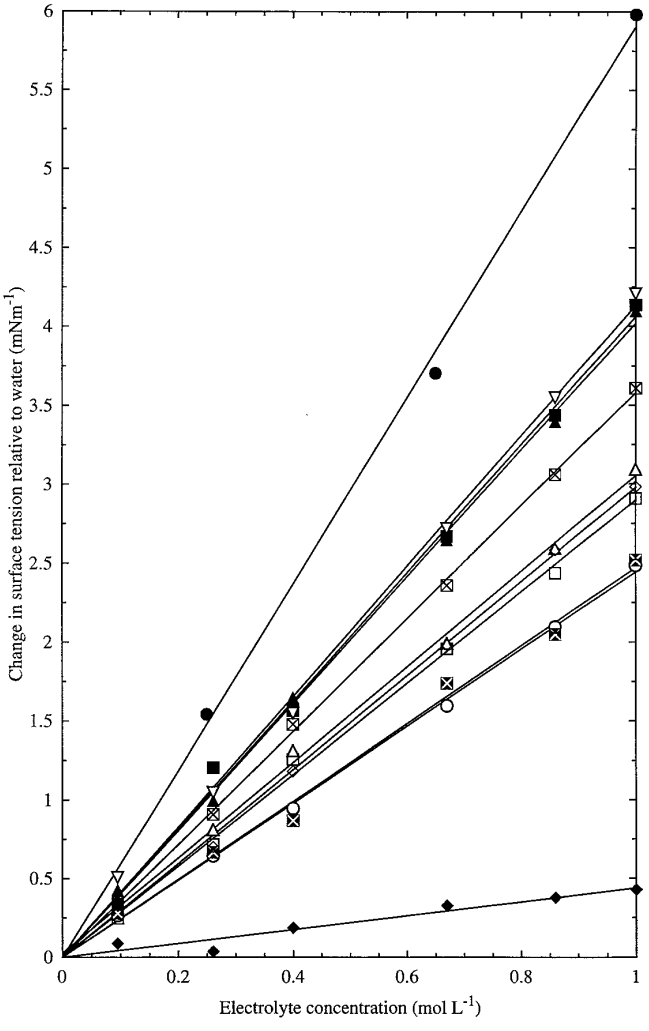

FIG. 4. Effect of electrolyte concentration on the change in surface tension relative to water for electrolytes containing multivalent ions. Bubble interval, 1.5 s. Experimental error in data points is ±0.1 mN m^{-1}. $MgCl_2$ (■), $CaCl_2$ (▲), $LaCl_3$ (●), H_2SO_4 (♦), Li_2SO_4 (⊠), Na_2SO_4 (□), Cs_2SO_4 (△), $MgSO_4$ (○), $Mg(NO_3)_2$ (◇), $Ca(NO_3)_2$ (⊠), $Cr(NO_3)_3$ (▽).

TABLE 2
$d(\Delta\gamma)/dc$ for All Electrolytes Measured at Bubble Intervals 1.5 and 0.15 s, and Literature Values Were Available.

	$d(\Delta\gamma)/dc$		
Electrolyte	at 1.5 s	literature	at 0.15 s
HCl	−0.27 ± 0.04[a]	−0.29	0.11 ± 0.08
LiCl	1.98 ± 0.09	1.63	2.20 ± 0.05
NaCl	2.08 ± 0.08	1.55	2.10 ± 0.05
KCl	1.85 ± 0.05	1.60, 1.65	1.84 ± 0.10
CsCl	1.52 ± 0.07	1.56	1.60 ± 0.10
NH_4Cl	1.59 ± 0.09	1.34	1.66 ± 0.05
$(CH_3)_4NCl$	0.94 ± 0.03	0.6	1.42 ± 0.03
$MgCl_2$	4.06 ± 0.10	3.14[20]	4.31 ± 0.20
$CaCl_2$	4.02 ± 0.08	3.22	4.09 ± 0.20
$LaCl_3$	5.91 ± 0.30	4.73	6.59 ± 0.30
H_2SO_4	0.44 ± 0.06	0.64	0.59 ± 0.08
Li_2SO_4	3.58 ± 0.05	2.68[18]	4.58 ± 0.13
Na_2SO_4	2.90 ± 0.08	2.96	3.53 ± 0.06
Cs_2SO_4	3.02 ± 0.07	na[b]	3.44 ± 0.07
$MgSO_4$	2.44 ± 0.05	2.24[10]	3.13 ± 0.05
HNO_3	−0.83 ± 0.10	−0.70	−0.88 ± 0.09
NH_4NO_3	1.15 ± 0.04	2.06[20]	1.34 ± 0.07
$Mg(NO_3)_2$	2.98 ± 0.07	na	3.39 ± 0.11
$Ca(NO_3)_2$	2.47 ± 0.11	na	3.09 ± 0.03
$Cr(NO_3)_3$	4.13 ± 0.10	na	4.63 ± 0.30
$HClO_4$	−2.15 ± 0.08	−1.64	−2.12 ± 0.10
$LiClO_4$	0.27 ± 0.06	na	0.43 ± 0.03
$NaClO_4$	0.22 ± 0.06	0.73	0.50 ± 0.05
CH_3COOH	−38 ± 1[c]	na	41 ± 1
CH_3COOLi	0.84 ± 0.05	na	1.42 ± 0.06
CH_3COONa	0.93 ± 0.03	0.54	1.44 ± 0.07
CH_3COOK	0.76 ± 0.09[d]	0.45	1.18 ± 0.11[d]
CH_3COOCs	1.12 ± 0.10[d]	na	1.53 ± 0.13[d]
$(CH_3COO)_2Mg$	0.48 ± 0.07[d]	na	2.23 ± 0.04[d]
$CH_3COO(CH_3)_4N$	−0.51 ± 0.09	na	nd[b]
H_3PO_4	0.85 ± 0.06	0.98	1.19 ± 0.03
NaI	1.23 ± 0.06	1.45, 1.21	1.44 ± 0.08
NaBr	1.83 ± 0.05	1.97	1.89 ± 0.03
NaF	1.83 ± 0.06	na	2.34 ± 0.06
$NaClO_3$	0.89 ± 0.05	0.57[15]	0.95 ± 0.04
KOH	1.98 ± 0.04	1.77[17]	2.06 ± 0.03

Note. Temperature for experimental values was between 21 and 28°C, temperature for any one electrolyte within ±0.2°C. Note the dependence of $d(\Delta\gamma)/dc$ on temperature between 20 and 30°C is within experimental error, e.g., based on literature data (1) for KCl $d(\Delta\gamma)/dc$ at 20°C is 1.56 and at 30°C it is 1.66. Literature values of $d(\Delta\gamma)/dc$ calculated from data compiled by Abramzon and Gaukhberg (1), except the second mentioned values for KCl, NaI (3), and $(CH_3)_4NCl$, CH_3COOK (16). Temperature for literature values is 25°C, unless specified in superscript.

[a] The ± error is the standard deviation of data points from the line of best fit. Experimental error in $d(\Delta\gamma)/dc$ was estimated to be ± 0.1.

[b] ''na'' means not available, and ''nd'' means not determined.

[c] Estimated over the range 0.01 to 0.095 *M*.

[d] Curved lines were obtained, and $d(\Delta\gamma)/dc$ was estimated based on linear fit to data.

indicated that constant surface deficiencies were obtained corresponding to the concentration at which linear behavior (constant $d(\Delta\gamma)/d \ln a$) was obtained in Fig. 5. The trends in surface deficiency in Fig. 6 were clear (increasing in the order $LiCl < KCl < MgCl_2 < LaCl_3$) and in accord with the original trends from $d(\Delta\gamma)/dc$ (Figs. 3 and 4, Table 2). However, it must be noted that some resolution was lost in distinguishing between electrolytes in terms of $\Gamma_{el^2}^{H_2O}$ compared to $d(\Delta\gamma)/dc$. This was simply due to the accumulation of mathematical/experimental errors and theoretical assumptions in converting from concentration (M) to activities and then to surface deficiencies.

Using the experimental results it was also found of interest to express the molar concentration as Debye length ($1/\kappa$, thickness of the diffuse electrical double layer) and re-plot as $\Delta\gamma$ versus Debye length (Fig. 7). From this data it can be seen that $\Delta\gamma$ scales roughly with Debye length for all

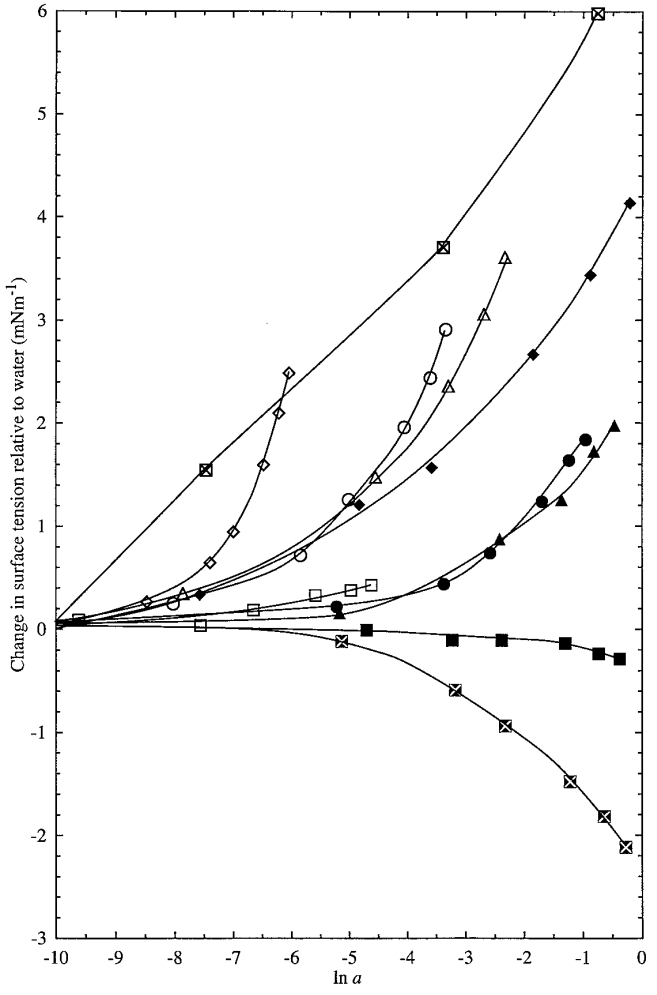

FIG. 5. Effect of electrolyte activity (as ln a) on the change in surface tension relative to water ($\Delta\gamma$). HCl (■), LiCl (▲), KCl (●), $MgCl_2$ (♦), $LaCl_3$ (⊠), H_2SO_4 (□), Li_2SO_4 (△), Na_2SO_4 (○), $MgSO_4$ (◇), $HClO_4$ (⊠).

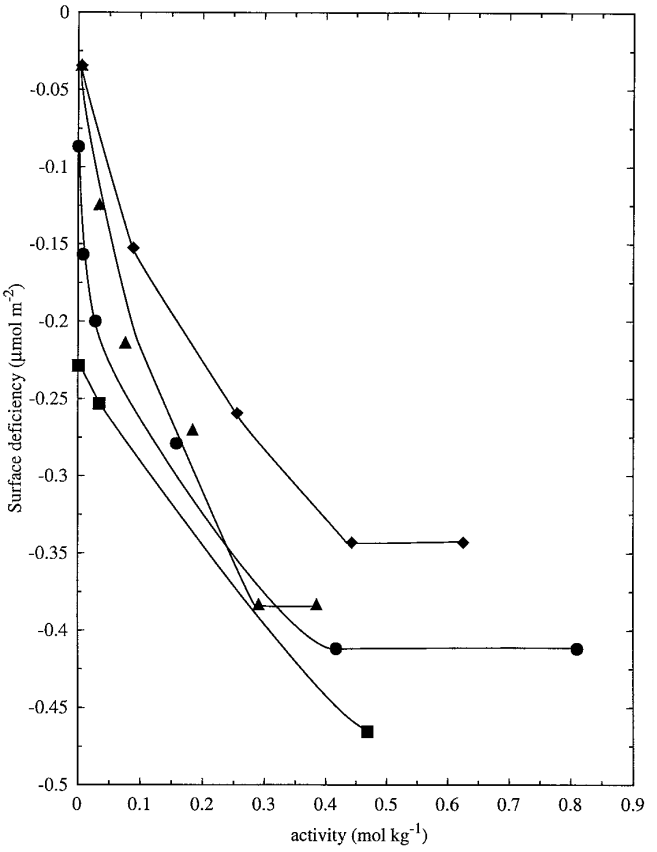

FIG. 6. Surface deficiency as a function of electrolyte activity for LiCl (♦), KCl (▲), $MgCl_2$ (●), and $LaCl_3$ (■).

electrolytes and for cations with the same counter-anion the correlation between $\Delta\gamma$ and Debye length is striking (Figs. 7b–d). This is clear evidence that electrostatic forces (and therefore image forces) make a major contribution to the surface tension of aqueous electrolyte solutions (supporting the fundamental basis for the Onsager–Samaras theory (7)). Perhaps more importantly, all electrolytes appear to merge asymptotically at a Debye length of approximately 0.1–0.2 nm. [We note that the meaning of Debye length is questionable at these high concentrations (above 1 M) where the size of hydrated ions is comparable to the classical Debye length calculated assuming the ions to be point charges.]

Correlation between $d(\Delta\gamma)/dc$, Entropy of Ion Hydration, and Jones–Dole Viscosity Coefficients

To further rationalize the trends in $d(\Delta\gamma)/dc$, the standard molar entropies of hydration of the counter-cations (19) for the chloride electrolytes were plotted against $d(\Delta\gamma)/dc$. Figure 8 shows a very good correlation between $d(\Delta\gamma)/dc$ and entropy of hydration. Entropy of hydration is indicative and a sensitive measure of the quantity of water molecules associated with an ion. Small ions of high valency are highly hydrated, increase the organization of water mole-

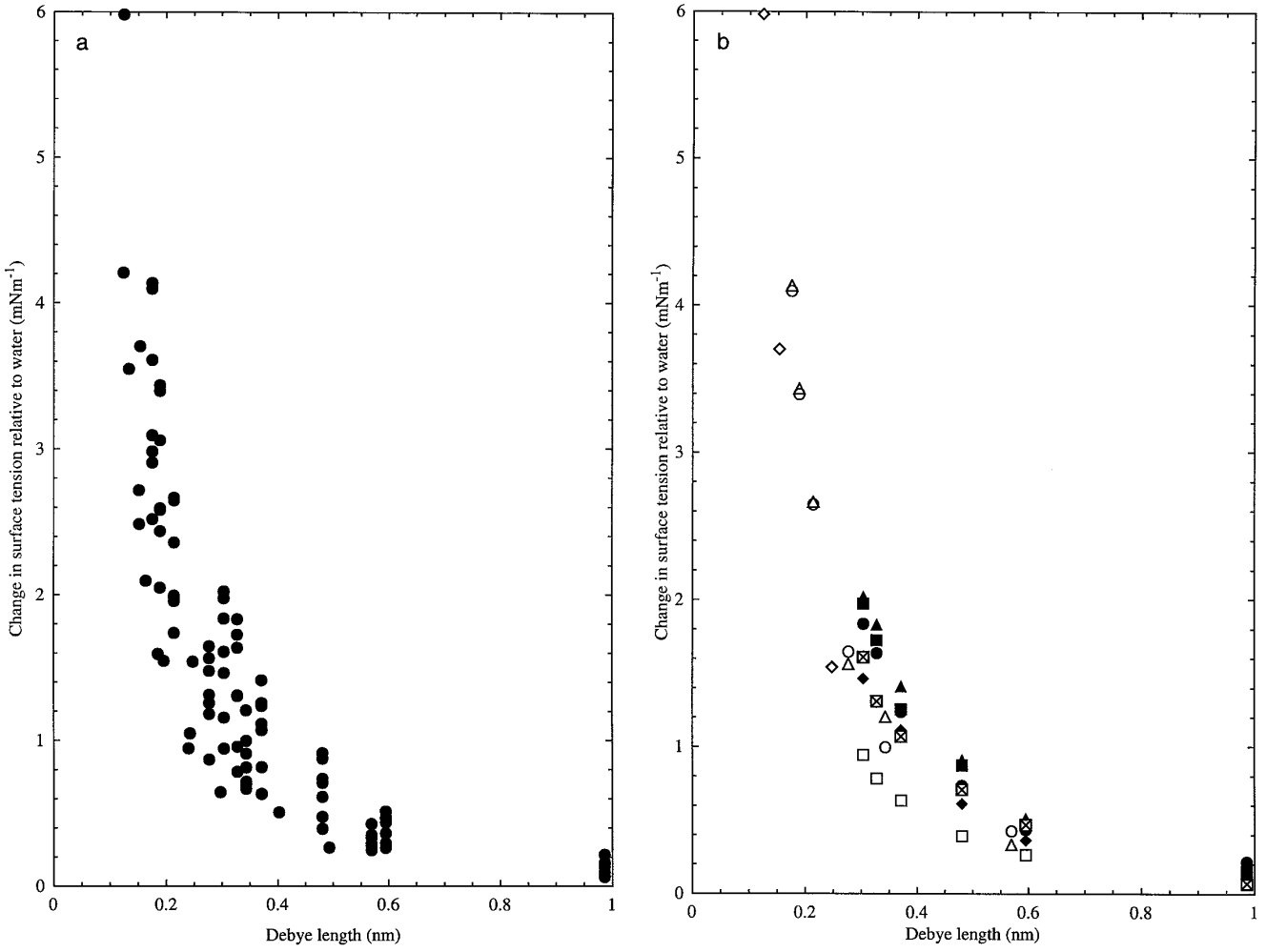

FIG. 7. (a) Effect of Debye length for selected electrolytes on the change in surface tension relative to water ($\Delta\gamma$). Electrolytes plotted: LiCl, NaCl, KCl, CsCl, NH_4Cl, $(CH_3)_4NCl$, $MgCl_2$, $CaCl_2$, $LaCl_3$, $NH_4(NO_3)$, $Mg(NO_3)_2$, $Ca(NO_3)_2$, $Cr(NO_3)_3$, Li_2SO_4, Na_2SO_4, Cs_2SO_4, $MgSO_4$. (b) Effect of Debye length for selected chloride electrolytes on the change in surface tension relative to water ($\Delta\gamma$). LiCl (■), NaCl (▲), KCl (●), CsCl (♦), NH_4Cl (⊠), $(CH_3)_4NCl$ (□), $MgCl_2$ (△), $CaCl_2$ (○), $LaCl_3$ (◇). (c) Effect of Debye length for selected nitrate electrolytes on the change in surface tension relative to water ($\Delta\gamma$). $NH_4(NO_3)$ (■), $Mg(NO_3)_2$ (▲), $Ca(NO_3)_2$ (●), $Cr(NO_3)_3$ (♦). (d) Effect of Debye length for selected sulfate electrolytes on the change in surface tension relative to water ($\Delta\gamma$). Li_2SO_4 (■), Na_2SO_4 (▲), Cs_2SO_4 (●), $MgSO_4$ (♦).

cules by compacting water molecules around themselves, have negative or low standard molar entropies of hydration and are commonly called structure-making ions. Large ions of low valency are weakly hydrated, have the opposite effect on water structure and are commonly called structure-breaking ions.

It is readily apparent from Fig. 8 that cations (as chloride salts) which are strongly hydrated (La^{3+}, Ca^{2+}, and Mg^{2+}) have high values of $d(\Delta\gamma)/dc$ and cations (as chloride salts) which are weakly hydrated (NH_4^+ and Cs^+) have low values of $d(\Delta\gamma)/dc$. All of these ions, in effect, displace water molecules from the gas/water interface and thereby increase surface tension, the magnitude being dependent on the extent of hydration. The negative adsorption of strongly hydrated cations (and anions) from the interface can thus be explained by the hydration Gibbs energy (the correlation between hydration Gibbs energy and $d(\Delta\gamma)/dc$ is 0.98; however, entropy data was used because the it is more reliable (19)) dominating the free energy required for a ''bare'' or ''partially bare'' ion to exist in the bulk solution or at the interface.

It is also interesting to note that the asymptotic mergence of Debye length with $\Delta\gamma$ at 0.1–0.3 nm ($\sim$1 M) is slightly less than the diameter of the fully hydrated ions (e.g., Li^+ 0.38 nm, Mg^{2+} 0.43 nm, Cl^- 0.33 nm) (20). The asymptotic mergence at 0.1–0.3 nm could also be due to the presence of an electrolyte free water layer at the interface (note the diameter of the water molecule is 0.28 nm), deficiencies in double layer theory applied to bubbles and the consequent meaning of Debye length at the high (1 M) electrolyte concentrations where the mergence occurs.

An alternative approach to the effects of ions on water

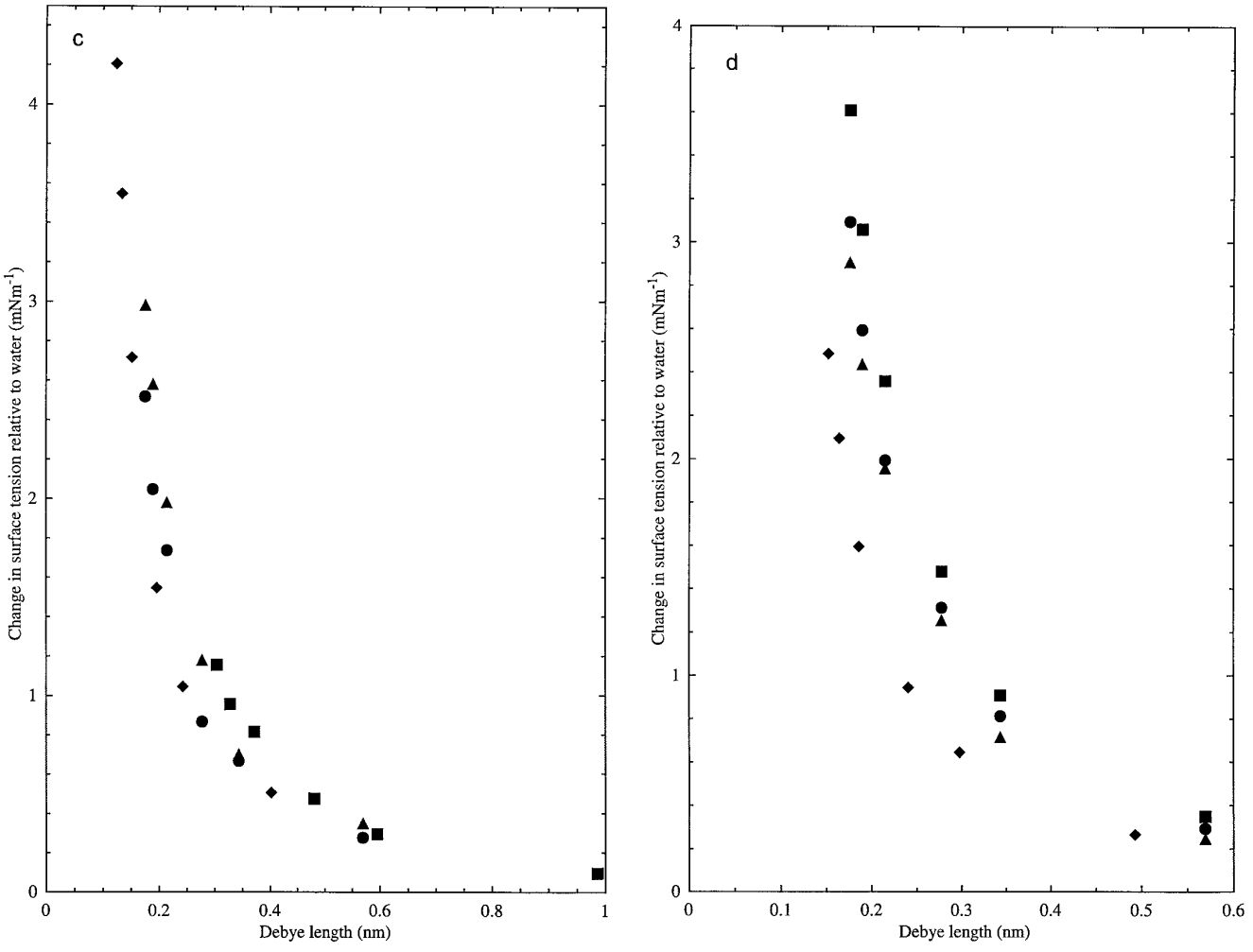

FIG. 7—*Continued*

structure, independent of entropy of ion hydration, involves the effects of electrolyte concentration on solution viscosity. It was shown earlier that viscosity influences the measurement of surface tension at short bubble intervals (Fig. 2). Electrolyte solutions with relatively high viscosity also contain a cation and/or anion which are highly hydrated (e.g., $MgSO_4$) and hence viscosity and ionic hydration are interrelated. Jones and Dole (21) have shown that the increase in viscosity of electrolyte solution with concentration, relative to water, follows the expression:

$$\eta/\eta_w = 1 + A\sqrt{c} + Bc + \ldots, \qquad [2]$$

where η is viscosity of the electrolyte solution of concentration c and η_w is viscosity of water. The coefficient A is due to interionic forces (electrostatic) which maintain a space lattice structure of the electrolyte, and the coefficient B (the so-called Jones–Dole or viscosity B coefficient) is representative of the retardation of solution flow due to hydration of ions. Structure making ions have positive values of B and structure breaking ions have negative values (19, 22). The correlation between B and $d(\Delta\gamma)/dc$ is shown in Fig. 9 and was 0.86. This correlation is weaker compared to that between entropy of ion hydration and $d(\Delta\gamma)/dc$ (0.94). Nevertheless, the fact that two such independent measures of ion hydration correlate with $d(\Delta\gamma)/dc$ is strong evidence for a link between surface tension and water structure.

Effect of Electrolyte Concentration on Dissolved Oxygen Solubility and Correlation with $d(\Delta\gamma)/dc$

Figure 10 shows the effect of concentration of some selected chloride electrolytes on the solubility of oxygen in aqueous solution. Oxygen solubility decreases exponentially with increasing electrolyte concentration. For mono-, di-, and tri-valent cations of chloride, sulfate, and nitrate electrolytes the solubility decreased in the order 1:1 > 1:2 > 1:3. Within any group (e.g., 1:1) there is no significant change in oxygen solubility for different cations, but Li^+ cations

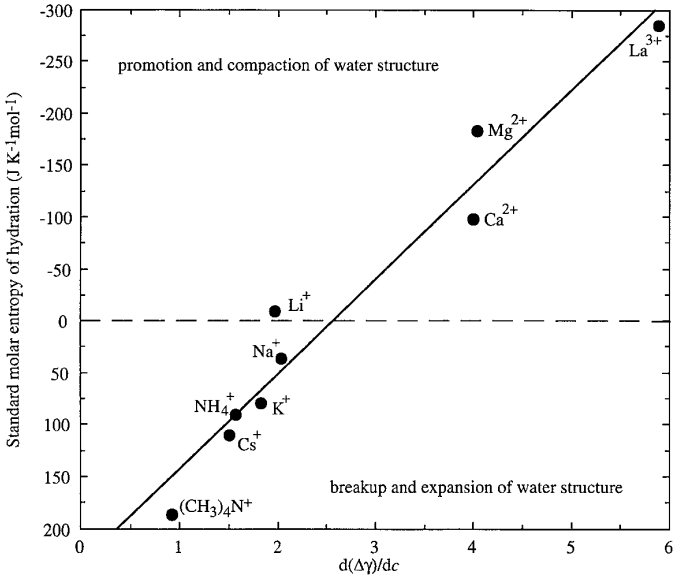

FIG. 8. Correlation between standard molar entropies of hydration of cations as chloride solutions (19) and $d(\Delta\gamma)/dc$. Correlation coefficient = 0.94.

seem to have consistently the least effect. The mineral acids had the least effect on oxygen solubility. Figure 10 showed a rapid decrease in oxygen solubility in going from a bulk electrolyte concentration of 0 to 2 *M*. Our $d(\Delta\gamma)/dc$ values are based on plots of $\Delta\gamma$ versus bulk concentrations in the range 0.05 to 1 *M* (Figs. 3 and 4). For chloride electrolytes common to our surface tension measurements a plot of the exponential decay coefficient for oxygen solubility versus

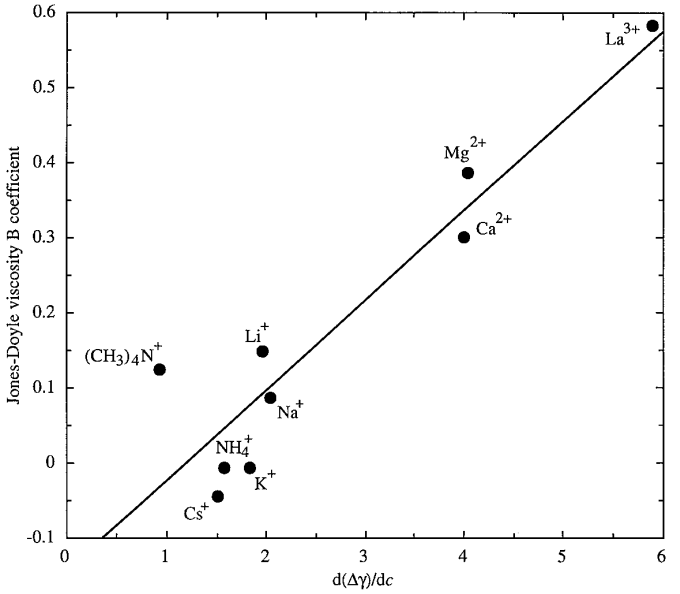

FIG. 9. Correlation between Jones–Dole viscosity coefficient, *B* (19, 22), and $d(\Delta\gamma)/dc$. Correlation coefficient = 0.86.

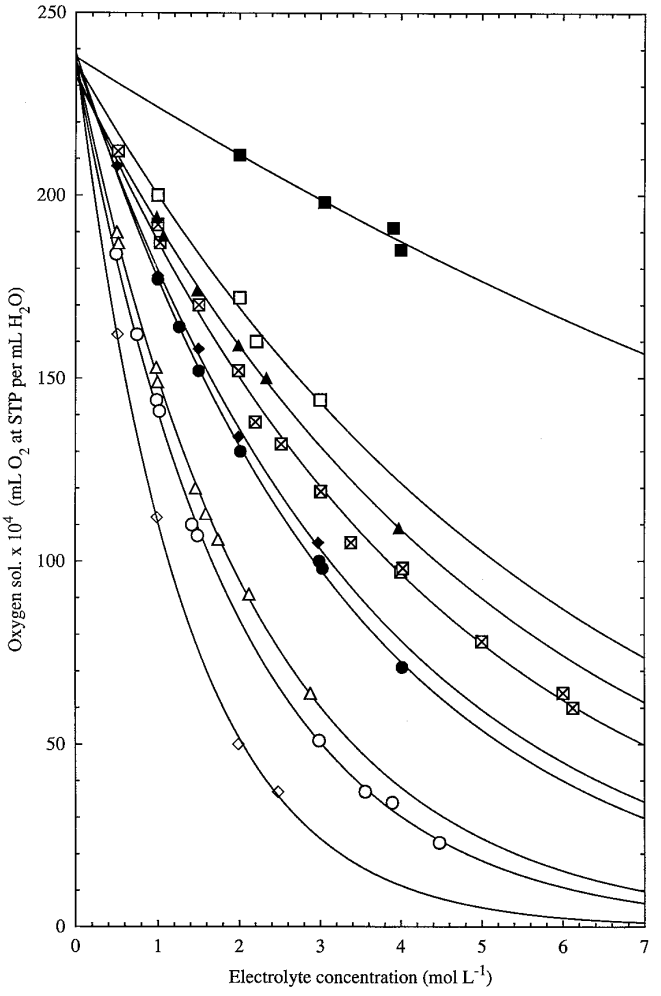

FIG. 10. Effect of electrolyte concentration (as chloride solutions) on the solubility of oxygen in water (Bunsen coefficients) at 37°C. Solubility of oxygen in pure water is 0.0240 mL O_2 at STP per mL H_2O. Solubility data taken from ref. (13). Exponential curve fit with decay coefficients given in brackets: HCl (■) (−0.06), LiCl (▲) (−0.19), NaCl (●) (−0.30), KCl (♦) (−0.28), CsCl (⊠) (−0.22), NH_4Cl (□) (−0.17), $MgCl_2$ (△) (−0.46), $CaCl_2$ (○) (−0.51), $LaCl_3$ (◇) (−0.76).

$d(\Delta\gamma)/dc$ gave a straight line with correlation coefficient of 0.96 (Fig. 11).

Sakai (23) has reported on the variation in relative concentration of ions as a function of relative distance from a bubble surface. The procedure involved analysing layers of solution around a small bubble (0.30 to 1.40 mm in diameter) in an aqueous solution of 0.005 *M* $MgCl_2$. The sampling of successive layers of relative thickness around the bubble (based on an ''onion-like'' structure) was via the jet drop method. Experimental results showed that at a relative distance of 0.2 (the distance for the bulk concentration is taken as 1.0) from the interface, the Mg^{2+} concentration was at least 2 times higher than the bulk concentration. For shorter distances the Mg^{2+} concentration is at least 3 times larger. Similarly Irsavechilli (20) has calculated (based on the

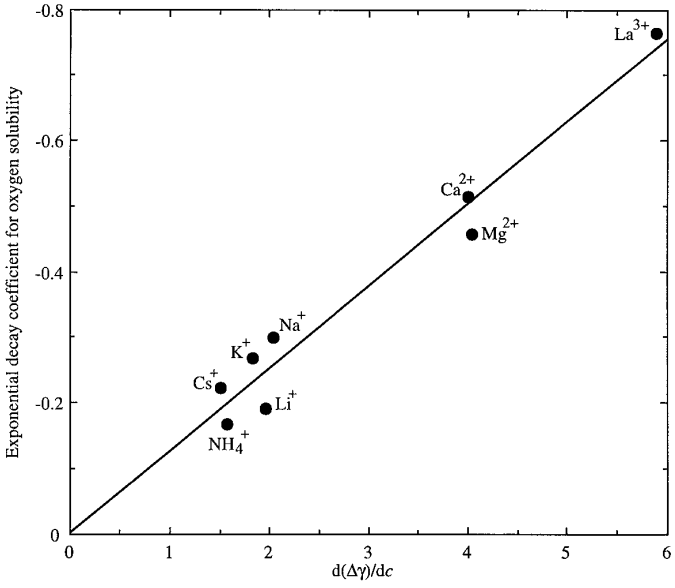

FIG. 11. Correlation between exponential decay coefficient for oxygen solubility in cationic chloride solutions and $d(\Delta\gamma)/dc$. Correlation coefficient = 0.96.

Boltzmann distribution of ions) the ion density profile for a 1:1 electrolyte of bulk concentration 0.1 *M* at a charged surface (charge density = -0.0621 Cm^{-2} and potential -66.2 mV). Note the ζ potential at the air-deionized water interface has recently been established to be -65 mV (24). At the surface the cation and anion concentrations are approximately 1.3 and 0 *M,* respectively, and at 0.96 nm (Debye length) the concentrations are approximately 0.25 and 0.05 *M,* respectively. On the basis of these results, the electrolyte concentration within the electrical double layer, in our case, would be many times greater than the bulk concentration (0.05 to 1 *M*). These concentrations are in the region were the oxygen solubility is at least 2–3 times less than for the bulk concentration.

Neither of the above predictions of electrolyte concentration within the electrical double layer consider the model of an electrolyte or ion free layer of water at the interface. Sakai (23) used a very low concentration of $MgCl_2$ (0.005 *M*), at which the presence of a model water free layer is unlikely. Obviously, the probability of such a layer existing increases with electrolyte concentration and there possibly exists a critical concentration at which the layer forms. The model based on a distinct ion free layer at the gas/electrolyte solution interface is clearly crude. Instead, it is more probable that the ion concentration profile from the gas/electrolyte solution interface is complex and may even go through several abrupt oscillations before the bulk ion concentration is reached (25, 26). It therefore may be more appropriate to talk in terms of concentration gradients or fluctuations of dissolved gases and electrolyte concentration gradients in the region of the bubble surface.

The existence of submicroscopic gas bubbles and clusters thereof in water and electrolyte solutions between hydrophobic and hydrophilic surfaces has recently been investigated by inducing optical cavitation via a laser (27). The submicroscopic bubbles have been coined ''bubstons'' (meaning bubbles stabilized by ions) and were believed to have diameters of approximately 1–10 nm. The mere fact that submicroscopic bubbles in electrolyte solution have been detected lends support to the possibility that the concentration gradient or fluctuations of dissolved gas near the macroscopic bubble surface has some influence on surface tension and even the interaction between surfaces or bubbles. We suggest this is inherently related to the hydration of ions and consequent alteration of water structure. Highly hydrated ions cause compaction of water molecules and a reduction in the number of microscopic gas bubbles. Thus, it is not surprising that a correlation exists between $d(\Delta\gamma)/dc$ and entropy of hydration and oxygen solubility.

While in the present study we have investigated a wide range of chloride electrolytes and found a good correlation between surface tension, entropy of hydration and dissolved gas concentration; other electrolytes need to be investigated. In order to compare electrolytes with no common ions such as NaCl versus $LiNO_3$, ion-pairing forces must be taken into account. Once an improved theoretical understanding of ion-pairing forces and effects on water structure has been developed, correlations such as we have reported should be able to be explained more clearly. Unfortunately, existing theories on the behaviour of electrolytes at interfaces do not consider changes in water structure or dissolved gas concentration in the double layer compared to water in the bulk solution.

RELATIONSHIP BETWEEN d($\Delta\gamma$)/dc AND BUBBLE COALESCENCE

The ability for most inorganic electrolytes to inhibit the coalescence of gas bubbles above a critical concentration has been carefully studied in both recent and early literature (12, 28). This has been attributed to the Gibbs–Marangoni effect/surface elasticity (16, 29), hydration repulsive forces (30), electrical repulsive forces (31), and a reduction in the hydrophobic attraction (12). In a subsequent paper (32) we will discuss a possible hydrodynamic interaction between bubbles in electrolyte solution based on work in progress using the molecular analysis of surface interaction forces (MASIF) technique (33).

Predicted Film Rupture Thicknesses for Two Coalescing Bubbles and the Gibbs–Marangoni Effect

The Gibbs–Marangoni effect/surface elasticity arises from surface tension gradients ($d(\Delta\gamma)/dc$) formed during expansion or contraction of bubbles. The surface tension

gradients cause movement of molecules or ions to, from, and along the gas/water interface. The viscous drag from the ''moving'' interface produces an appreciable amount of underlying liquid to flow back into the film resulting in a restoration in thickness of the thinning lamella. It is well established that this mechanism is primarily responsible for bubble/foam stability induced by conventional surfactants. To test if the Gibbs–Marangoni effect can explain the inhibition of coalescence by simple electrolytes, we have as an initial attempt predicted the critical film rupture thicknesses for two coalescing bubbles based on the results of Cain and Lee (34) and the theory of Lee and Meyrick (35).

As two bubbles approach each other a plane circular film is formed between them. As the film thins and the bubbles get closer there is rapid stretching of the bubble/water interfaces. This causes a difference in surface tension values between the unstretched regions lying outside the film and the stretched regions within the film. The stretching accelerates until a film thickness (h) is reached where either compensation occurs due to Gibbs–Marangoni flow or the film ruptures. The film thickness where stretching starts to decelerate (or where drainage is compensated by the surface tension differences) was denoted by Cain and Lee (34) as the ''arrest'' thickness (h_{arr}) and corresponds to an ''arrest'' surface tension difference ($\Delta\gamma_{arr}$). The arrest thickness and arrest surface tension can be related by (35)

$$h_{arr} = \frac{2c_o\phi}{\upsilon\Delta\gamma_{arr}RT}\left(\frac{d\gamma}{dc}\right)^2, \qquad [3]$$

where c_o is the bulk electrolyte concentration, ϕ is a factor incorporating the activity coefficient to convert between activity and molality, υ is the number of ions produced upon dissociation of the electrolyte, R is the gas constant, T is temperature, and $d(\Delta\gamma)/dc$ is the surface tension gradient. Equation [3] is a quantitative expression describing the surface elasticity of the film. Details of the theoretical background and derivation of the equation are given in the appendix.

Cain and Lee (34) carefully measured the drainage and rupture of films formed between two captive bubbles in KCl solution. Film thicknesses were measured by an optical interference method using a He–Ne laser and microscopes. Rupture thicknesses in 1.0 *M* solutions were between 55 and 75 nm, with a film drainage time of ~600 ms. In 0.5 *M* solution, the thicknesses were between 75 and 95 nm with drainage time ~420 ms. Lessard and Zieminski (28) studied the coalescence of two captive bubbles using similar bubble formation apparatus to Cain and Lee (34) and obtained a transition concentration (the concentration at which 50% of the bubbles do not coalesce) in KCl of 0.23 *M*. On the basis of the rupture thicknesses obtained by Cain and Lee (34), the rupture thickness in 0.23 M KCl would be, by extrapolation, in the region of 96 nm. Cain and Lee (34) went on to correctly assume that the arrest thickness (h_{arr}) at the bubble coalescence transition concentration was equal to the rupture thickness (h_{rup}). In other words, at the bubble coalescence transition concentration, 50% of bubbles do not coalesce at thickness $h = h_{arr}$ and 50% do coalesce at the same thickness $h = h_{rup}$. Hence from the rupture thickness in 0.23 *M* KCl and Eq. [3], the corresponding rupture surface tension difference in the film ($\Delta\gamma_{rup}$) at which film drainage/coalescence is becoming inhibited can be calculated (since at the transition concentration $h_{arr} = h_{rup}$ then $\Delta\gamma_{arr} = \Delta\gamma_{rup}$). The value of $\Delta\gamma_{rup}$ is taken as the surface tension at the interface at the narrowest point of the film between two bubbles minus surface tension at the interface for a single bubble.

The calculation of $\Delta\gamma_{rup}$ yields a value of 0.0037 mN m^{-1}. Assuming this value is valid for all electrolytes (that is the mechanism of film formation and eventual rupture is the same for all electrolytes), then by application of Eq. [3] the rupture film thicknesses can be calculated for any electrolyte provided that the transition concentrations and $d(\Delta\gamma)/dc$ values are known. The $d(\Delta\gamma)/dc$ values for a large range of electrolytes were given in Table 2 and transition concentrations for some of these electrolytes were given by Lessard and Zieminski (28). In Table 3 the results of the calculations are presented with the predicted film rupture thicknesses for two coalescencing bubbles shown in the last column.

Accepting any deficiencies in the theory on which the calculation of $\Delta\gamma_{rup}$ was based (for example, the dependence on rate of approach of bubbles appears not to have been taken into account) and that the magnitude of $\Delta\gamma_{rup}$ may even be 10–100-fold more, it is still inconceivable that such small surface tension differences in the film could generate sufficient flow of liquid to slow film drainage/rupture and

TABLE 3

Predicted Film Rupture Thicknesses (h_{rup}) for Two Coalescing Bubbles Attached to Capillaries, Relative to Results for KCl Obtained by Cain and Lee (34)

Electrolyte	Transition conc. TC (*M*)	$d(\Delta\gamma)/dc$	ϕ	ν	h_{rup} (nm)
$MgSO_4$	0.032	2.44	1.96	2	41
$MgCl_2$	0.055	4.06	0.89	3	58
$CaCl_2$	0.055	4.02	1.02	3	66
Na_2SO_4	0.061	2.90	1.53	3	57
LiCl	0.16	1.98	1.01	2	69
NaCl	0.175	2.08	1.08	2	89
NaBr	0.22	1.83	1.06	2	85
KCl	0.23	1.85	1.12	2	96

Note. The rupture surface tension difference in the film ($\Delta\gamma_{rup}$) at the transition concentration was calculated to be 0.0037 mN m^{-1} and used in the calcution of h_{rup} for all electrolytes. Transition concentrations taken from Lessard and Zieminski (28).

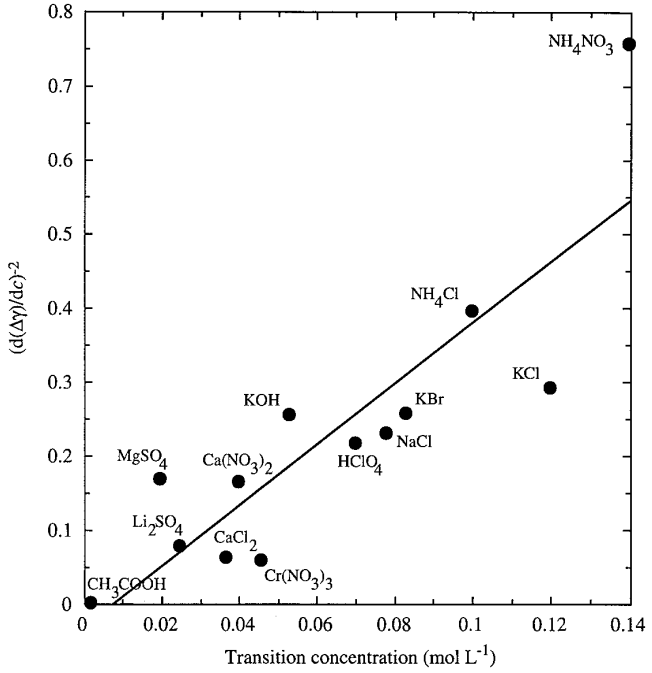

FIG. 12. Correlation between $[d(\Delta\gamma)/dc]^{-2}$ and bubble coalescence transition concentration taken from Craig *et al.* (12). Correlation coefficient = 0.74. Transition concentration was defined as the electrolyte concentration at which 50% coalescence occurs, on a scale where 100% coalescence is for water and 0% coalescence is where no further change in coalescence is measured with increasing electrolyte concentration. Hofmeier *et al.* (29) have since shown that the so-called transition concentration is due to a combination of the initial size of the bubbles emerging from the frit, bubble coalescence, and bursting of larger bubbles to form smaller bubbles.

bubble coalescence. Significantly larger values of $d(\Delta\gamma)/dc$ are required (a ''typical'' surfactant has a $d\gamma/dc$ of over -200; note that CH_3COOH used in this study had a $d(\Delta\gamma)/dc$ of -38) to give larger values of $\Delta\gamma_{arr}$, suggesting that the change in surface tension gradients produced by electrolytes at their transition concentrations are too weak to cause any significant Gibbs–Marangoni effects.

Further, we plotted $[d(\Delta\gamma)/dc]^{-2}$ versus the bubble coalescence transition electrolyte concentrations from Craig *et al.* (12) (Fig. 12). Such a plot is a test for the Gibbs–Marangoni effect and is based on Gibbs surface elasticity and the theory of Prince and Blanch relating $d(\Delta\gamma)/dc$ and transition concentrations (29, 36). The mediocre correlation coefficient (0.74) confirms that the inhibition of bubble coalescence caused by electrolytes is not just due to Gibbs–Marangoni effects (10). The correlation is significantly worse when deviant salts such as $CH_3COO(CH_3)_4N$ and others with low values of $d(\Delta\gamma)/dc$ are plotted. Below we discuss other possible mechanisms which may influence bubble coalescence.

Hydration Repulsive Forces

Pashley (30) has given good evidence that hydration forces may be operative between bubbles if film thicknesses of approximately 5 nm or less were obtained. This may be possible at high electrolyte concentration (>1 *M*) where rupture thicknesses are expected to be much thinner than those obtained by Cain and Lee (34) and shown in Table 3.

Interestingly, Tsao and Koch (37) also favoured a non-hydrodynamic repulsive force and alluded to the hydration force as the mechanism of inhibition of coalescence. They showed visible (video images) evidence of a bubble rising in 0.4 *M* NaCl and bouncing off a secondary bubble fixed to a capillary. In pure water, no bouncing was observed and coalescence occurred. In the electrolyte solutions, Marangoni effects were ruled out as the reason for inhibition. Tsao and Koch (37) did not measure the film thickness between the bouncing bubbles but stated that the bubbles approach each other within a distance the order of the Debye length ($\sim$0.5 nm for 0.4 *M* NaCl), much closer than the experimentally measured thicknesses of Cain and Lee (34) ($\sim$85 nm for 0.5 *M* KCl). Obviously, at small enough thicknesses a repulsive force, perhaps a hydration force becomes significant. To fully explain the bouncing phenomena, surface deformation (flattening or dimpling) of bubbles were also considered.

The experimental rupture thicknesses obtained by Cain and Lee (34) and predicted thicknesses shown in Table 3 are for two bubbles fixed to capillaries. These thicknesses occur over distances approximately 10-fold longer than any conceivable range of a hydration force (38, 39). Hence for two fixed bubbles in electrolyte solution, the inhibition of bubble coalescence cannot be satisfactorily explained by hydration forces. For bouncing bubbles where a bubble rising under gravity (approach velocity $\sim$15 cm s^{-1}) colliding with a fixed bubble, very thin films may form due to inertial forces with bouncing occurring due to repulsive hydration forces and surface deformation (37). These results suggest that the forces encountered during the close approach of either two fixed bubbles, a fixed and a rising bubble, two rising (free) bubbles, or bubbles in a foam are likely to be very different and therefore different inhibition mechanisms may be operative. This would explain much of the disagreement over the mechanisms determining whether bouncing or coalescence occurs. Clearly, more experimental and theoretical research is required.

Interfacial Attraction Due to Microscopic Bubbles

The calculated relative film rupture thicknesses in Table 3 are much larger than the distances over which conceivable van der Waals, electrostatic, or hydration forces have any significant strength. Hence, at the rupture thickness these forces are too weak and cannot explain any attraction or repulsion between coalescing bubbles in electrolyte solutions. The one remaining surface force which may significantly override any other forces which coalescing bubbles

rising in solution experience as a function of distance is the so-called attractive hydrophobic force. Using surface force techniques, researchers have obtained conflicting results on the effect of electrolytes on the attraction between hydrophobic surfaces. This now seems to have been resolved by Wood and Sharma (40). They give very good evidence that the range of the interaction between hydrophobic surfaces depends on the way in which the surfaces are prepared. For example, a patchwise hydrophobic coating on mica gives a relatively long range attraction that is dependent on electrolyte concentration; whereas, mica fully coated with octadecyltriethoxysilane and characterised to be ''truly'' hydrophobic gives a much shorter range attraction (approximately 15 nm) independent of electrolyte concentration.

Based on the above results of Wood and Sharma (40), it is difficult support the original idea that the inhibition of bubble coalescence with increasing electrolyte concentration is due to a decrease in the then so-called hydrophobic attraction (10, 12). Instead, attention is now focused towards the role of dissolved gases on the specific interaction between air bubbles in electrolyte solution. The correlation between $d(\Delta\gamma)/dc$, entropy of ion hydration (Fig. 8) and Jones–Dole viscosity coefficients (Fig. 9) suggests that the mechanism of the interfacial attraction between bubbles may be due to some form of perturbation of water structure. This perturbation may be related to the effect of electrolyte concentration on dissolved gas concentration and therefore $d(\Delta\gamma)/dc$ and transition electrolyte concentration for bubble coalescence (10). This leads us to speculate that the attraction between bubbles operates through some form of microscopic bubble interaction or bridging between the macroscopic bubbles, just as has been similarly reported for solid hydrophobic surfaces and referred to as bridging cavitation (40, 41). We argue that since the gas content of the water decreases with increasing electrolyte concentration so does the microscopic bubble concentration and this weakens the bridging attraction between macroscopic bubbles.

CONCLUSIONS

The surface tension/concentration gradients ($d(\Delta\gamma)/dc$) of aqueous solutions of electrolytes is directly proportional to the entropy of hydration of cations with a common anion. In general, highly hydrated cations and anions cause the greatest increase in surface tension, but the cation–anion pairing determines the actual change (increase, decrease, or no change) in surface tension. At the same time the Jones–Dole viscosity coefficients of cations correlate well with increasing $d(\Delta\gamma)/dc$. Both ion hydration and the viscosity coefficients are an indirect measure of water structure and hence a link between surface tension and water structure is obvious. The role of $d(\Delta\gamma)/dc$ and therefore the Gibbs–Marangoni effect in the inhibition of bubble coalescence by electrolytes is insignificant, and we argue that the presence of dissolved gases is a much more important aspect to consider. Electrolytes decrease the dissolved gas concentration (the decrease correlating well with $d(\Delta\gamma)/dc$ which in turn decreases the strength of the attraction between bubbles mediated by microbubbles and this inhibits coalescence.

APPENDIX

Calculation of Film Thickness

Lee and Meyrick (35) have derived the equation for the local surface tension in the film between coalescing gas bubbles in aqueous electrolyte solutions. The derivation is based on (i) the surface deficiency (negative adsorption) of electrolyte at the gas/water interface according to Gibbs's adsorption equation

$$\Gamma_{\text{el}}^{\text{H}_2\text{O}} = -\frac{1}{RT}\left(\frac{d\gamma}{d\ln a_{\text{el}}}\right)_T, \qquad [4]$$

where Γ is surface deficiency, γ is surface tension, R is the gas constant, T is temperature, and a_{el} is electrolyte activity, and (ii) change in equilibrium film thickness with electrolyte concentration in the film

$$\frac{dh}{dc} = \frac{h}{\Gamma}\frac{d\Gamma}{dc} + \frac{h^2}{2\Gamma}, \qquad [5]$$

where c is the electrolyte concentration in the film center and h is film thickness.

$d\Gamma/dc$ is approximated by

$$\frac{d\Gamma}{dc} = -\frac{1}{RT}\frac{d\gamma}{dc}\phi \quad \text{with } \phi = 1\Big/\left(1 + \frac{d(\ln f)}{d(\ln c)}\right), \qquad [6]$$

where ϕ is used to convert the activity, a_{el}, to concentration, c (as molality), using the slope of a plot of the natural log of the molal activity coefficient, f, versus the natural log of concentration, c (range 0.1 to 1 mol kg^{-1}). The value of $d(\ln f)/d(\ln c)$ with c expressed as molality was taken to be equal to the value of $d(\ln f)/d(\ln c)$ with c expressed as molarity. We calculated ϕ for each electrolyte in Table 3 using data from the literature (13, 17).

Equations [4] and [5] were combined and integrated with initial conditions of $h = \infty$ and $c = c_o$ to obtain an equation giving the concentration of electrolyte at any film thickness:

$$c = c_o\frac{h}{(h - 2\beta)} \quad \text{where } \beta = -\frac{d\Gamma}{dc}. \qquad [7]$$

β was assumed to be constant over the small range of c involved. Thus at a thickness h, the rise in γ (symbolized $\Delta\gamma_f$) is represented by the γ at the outside of the film

(equivalent to the γ for a single bubble) minus that at the center of the film and is equal to

$$\Delta\gamma_f = \left(\frac{d\gamma}{dc}\right)\Delta c = c_o\left(\frac{d\gamma}{dc}\right)\frac{2\beta}{(h-2\beta)}. \qquad [8]$$

For electrolytes, 2β is small compared to h. Resubstituting for β, simplifying and rearranging in terms of h gives

$$h = \frac{2c_o\phi}{\Delta\gamma_f RT}\left(\frac{d\gamma}{dc}\right)^2. \qquad [9]$$

Prince and Blanch (36) introduced a factor, υ, to account for the number of ions produced upon dissociation of the electrolyte. Thus the film thickness h for a given c_o can be calculated using

$$h = \frac{2c_o\phi}{\upsilon\Delta\gamma_f RT}\left(\frac{d\gamma}{dc}\right)^2. \qquad [10]$$

Equation [10] was used to calculate the thickness of the film at which rupture (h_{rup}) occurs at the transition electrolyte concentration, based on the calculated rupture $\Delta\gamma_f$ (equal to $\Delta\gamma_{rup}$) for KCl.

ACKNOWLEDGMENTS

We thank Associate Professor P. M. Claesson for critically reading and correcting the manuscript, Professor Barry Ninham for invaluable support and discussions, and professor Th. F. Tadros for stimulating discussions. Special thanks to the Wenner-Gren Foundation for a research award to P.K.W. and The Institute for Surface Chemistry for providing research facilities.

REFERENCES

1. Abramzon, A. A., and Gaukhberg, R. D., *Russian J. App. Chem.* **66**(6), 1139 (1993); Continued in **66**(7), 1315 and **66**(8), 1473 (1993).
2. Ralston, J., and Healy, T. W., *J. Colloid Interface Sci.* **42,** 629 (1973).
3. Johansson, K., and Eriksson, J. C., *J. Colloid Interface Sci.* **49,** 469 (1974).
4. Aveyard, R., and Saleem, S. M., *J. Chem. Soc. Faraday Trans. 1* **72,** 1609 (1976).
5. Hey, M. J., Shield, D. W., Speight, J. M., and Will, M., *J. Chem. Soc. Faraday Trans. 1* **77,** 123 (1981).
6. Adamson, A. W., ''Physical Chemistry of Surfaces,'' 5th ed., p. 83. Wiley, New York, 1990.
7. Onsager, L., and Samaras, N. N. T., *J. Chem. Phys.* **2,** 528 (1934).
8. Drost-Hansen, W., *Ind. Eng. Chem.* **57,** 18 (1965).
9. Horne, R. A., and Young, R. P., *Electrochim. Acta* **17,** 763 (1972).
10. Weissenborn, P. K., and Pugh, R. J., *Langmuir* **11,** 1422 (1995).
11. Mysels, K. J., *Colloids Surf.* **43,** 241 (1990).
12. Craig, V. S. J., Ninham, B. W., and Pashley, R. M., *J. Phys. Chem.* **97,** 10192 (1993).
13. Weast, R. C., Ed., ''CRC Handbook of Chemistry and Physics,'' 69th ed., F-33, D-219, D-272. CRC Press, Florida, 1988–1989.
14. Fainerman, V. B., Makievski, A. V., and Miller, R., *Colloids Surf. A: Phys. Eng. Aspects* **75,** 229 (1993).
15. Hiemenz, P. C., ''Principles of Colloid and Surface Chemistry,'' 2nd ed., p. 392. Dekker, New York, 1986.
16. Christenson, H. K., and Yaminsky, V. V., *J. Phys. Chem.* **99,** 10420 (1995).
17. Robinson, R. A., and Stokes, R. H., ''Electrolyte Solutions,'' 2nd ed., p. 24–33, 459, 491–504. Butterworths, London, 1959.
18. Lobo, V. M. M., and Quaresma, J. L., ''Handbook of Electrolyte Solutions.'' Elsevier, Amsterdam, 1989.
19. Lyklema, H., ''Fundamentals of Interface and Colloid Science, Volume I: Fundamentals,'' p. 5.37, 5.52. Academic Press, London, 1991.
20. Israelachvili, J., ''Intermolecular & Surface Forces,'' 2nd ed., p. 55, 110, 240. Academic Press, London, 1992.
21. Jones, G., and Dole, M., *J. Am. Chem. Soc.* **51,** 2950 (1929).
22. Marcus, Y., *J. Sol. Chem.* **23,** 831 (1994).
23. Sakai, M., *Prog. Colloid Polym. Sci.* **77,** 136 (1988).
24. Graciaa, A., Morel, G., Saulner, P., Lachaise, J., and Schechter, R. S., *J. Colloid Interface Sci.* **172,** 131 (1995).
25. Ennis, J., Kjellander, R., and Mitchell, J. D., *J. Chem. Phys.* **102,** 975 (1995).
26. Kjellander, R., *J. Phys. Chem.*, in press.
27. Vinogradova, O. I., Bunkin, N. F., Churaev, N. V., Kiseleva, O. A., Lobeyev, A. V., and Ninham, B. W., *J. Colloid Interface Sci.* **173,** 443 (1995).
28. Lessard, R. R., and Zieminski, S. A., *Ind. Eng. Chem. Fundam.* **10,** 260 (1971).
29. Hofmeier, U., Yaminsky, V. V., and Christenson, H. K., *J. Colloid Interface Sci.* **174,** 199 (1995).
30. Pashley, R. M., *J. Colloid Interface Sci.* **80,** 153 (1981).
31. Marrucci, G., and Nicodemo, L., *Chem. Eng. Sci.* **22,** 1257 (1967).
32. Weissenborn, P. K., Ederth, T., Claesson, P. M., and Pugh, R. J., to be submitted (1997).
33. Parker, J. L., *Prog. Surf. Sci.* **47,** 205 (1994).
34. Cain, F. W., and Lee, J. C., *J. Colloid Interface Sci.* **106,** 70 (1985).
35. Lee, J. C., and Meyrick, D. L., *Trans. Inst. Chem. Eng.* **48,** T37 (1970).
36. Prince, M. J., and Blanch, H. W., *AIChE J.* **36,** 1425 (1990).
37. Tsao, H-K., and Koch, D. L., *Phys. Fluids* **6,** 2591 (1994).
38. Pashley, R. M., and Quirk, J. P., *Colloids Surf.* **9,** 1 (1984).
39. Shubin, V. E., and Kékicheff, P., *J. Colloid Interface Sci.* **155,** 108 (1993).
40. Wood, J., and Sharma, R., *Langmuir* **11,** 4797 (1995).
41. Parker, J. L., Claesson, P. M., and Attard, P., *J. Phys. Chem.* **98,** 8468 (1994).